Cellular/Molecular

Mechanisms Underlying Desynchronization of Cholinergic-Evoked Thalamic Network Activity

Juan Diego Pita-Almenar,[1] Dinghui Yu,[2,3] Hui-Chen Lu,[2,3,4] and Michael Beierlein[1]

[1]Department of Neurobiology and Anatomy, University of Texas Medical School, Houston, Texas 77030, [2]The Cain Foundation Laboratories, Jan and Dan Duncan Neurological Research Institute at Texas Children's Hospital, [3]Department of Pediatrics, and [4]Program in Developmental Biology, Department of Neuroscience, Baylor College of Medicine, Houston, Texas 77030

Synchronous neuronal activity in the thalamocortical system is critical for a number of behaviorally relevant computations, but hypersynchrony can limit information coding and lead to epileptiform responses. In the somatosensory thalamus, afferent inputs are transformed by networks of reciprocally connected thalamocortical neurons in the ventrobasal nucleus (VB) and GABAergic neurons in the thalamic reticular nucleus (TRN). These networks can generate oscillatory activity, and studies *in vivo* and *in vitro* have suggested that thalamic oscillations are often accompanied by synchronous neuronal activity, in part mediated by widespread divergence and convergence of both reticulothalamic and thalamoreticular pathways, as well as by electrical synapses interconnecting TRN neurons. However, the functional organization of thalamic circuits and its role in shaping input-evoked activity patterns remain poorly understood. Here we show that optogenetic activation of cholinergic synaptic afferents evokes near-synchronous firing in mouse TRN neurons that is rapidly desynchronized in thalamic networks. We identify several mechanisms responsible for desynchronization: (1) shared inhibitory inputs in local VB neurons leading to asynchronous and imprecise rebound bursting; (2) TRN-mediated lateral inhibition that further desynchronizes firing in the VB; and (3) powerful yet sparse thalamoreticular connectivity that mediates re-excitation of the TRN but preserves asynchronous firing. Our findings reveal how distinct local circuit features interact to desynchronize thalamic network activity.

Key words: **basal forebrain; channelrhodopsin; lateral inhibition; oscillation; T-type calcium channel; thalamocortical**

Introduction

Acetylcholine (ACh) has long been implicated in a number of cognitive processes, including arousal, attention, learning, and the processing of sensory information, but the cellular mechanisms underlying cholinergic control remain poorly understood and controversial (Picciotto et al., 2012; Munoz and Rudy, 2014). Cholinergic neurons in the basal forebrain (BF; Zaborszky, 2002) and in the pedunculopontine/laterodorsal tegmental area of the brainstem (Woolf and Butcher, 2011) comprise two of the main sources of ACh in the brain. Although activation of cholinergic projection neurons in both areas is associated with behavioral states such as arousal that can last tens of seconds to minutes (Lee et al., 2005; Boucetta et al., 2014), cholinergic control of attention, sensory processing, and learning occur on timescales of tens of milliseconds to seconds (Parikh et al., 2007; Letzkus et al., 2011; Pinto et al., 2013). These roles appear incompatible with the traditional view of ACh as a global and slow-acting neuromodulator (Descarries et al., 1997). In fact, an increasing number of studies have shown that the synaptic release of ACh can generate rapid, precise, and highly local presynaptic and postsynaptic responses (Gu and Yakel, 2011; Arroyo et al., 2012; Sun et al., 2013; Munoz and Rudy, 2014), potentially allowing cholinergic systems to control local computations with high temporal precision (Chubykin et al., 2013). Therefore, it is critical to gain a better understanding of how cholinergic signaling influences activity patterns in neuronal circuits.

Here we examine the influence of cholinergic inputs on network activity of the somatosensory thalamus. Local thalamic networks are organized as reciprocally interconnected excitatory–inhibitory loops between glutamatergic neurons of the ventrobasal nucleus (VB) and GABAergic neurons of the thalamic reticular nucleus (TRN) (McCormick and Bal, 1997). The TRN is the only source of GABAergic input to VB cells and is thus intimately involved in gating sensory processing. The TRN also acts as a pacemaker for oscillatory thalamic activity, such as sleep spindles, by providing strong inhibition to thalamic nuclei that deinactivates low-threshold T-type Ca^{2+} channels in postsynaptic relay cells and results in the generation of Ca^{2+} spikes that can trigger bursts of action potentials (APs; Huguenard and McCormick, 2007). Studies performed *in vivo* and *in vitro* have concluded that oscillatory activity is accompanied by synchronized firing in populations of neurons, initiated by corticothalamic (CT) feedback and maintained by electrical synapses between

Received June 6, 2014; revised Aug. 29, 2014; accepted Sept. 13, 2014.

Author contributions: J.D.P.-A., D.Y., H.-C.L., and M.B. designed research; J.D.P.-A. and D.Y. performed research; J.D.P.-A., D.Y., H.-C.L., and M.B. analyzed data; J.D.P.-A., D.Y., H.-C.L., and M.B. wrote the paper.

This work was supported in part by National Institute of Neurological Disorders and Stroke Grants NS048884 (H-C.L. and D.Y.) and NS077989 (M.B.). We thank Drs. Adam Carter, Barry Connors, and Jay Gibson for comments on this manuscript and the Baylor Intellectual and Developmental Disabilities Research Center core facility (National Institutes of Health Grant HD024064) for confocal microscopy access.

The authors declare no competing financial interests.

Correspondence should be addressed to Michael Beierlein, Department of Neurobiology and Anatomy, University of Texas Medical School, 6431 Fannin, Suite 7.046, Houston, TX 77030. E-mail: michael.beierlein@uth.tmc.edu.

DOI:10.1523/JNEUROSCI.2321-14.2014

 0270-6474/14/3414463-12$15.00/0

TRN neurons and by the extensive synaptic divergence and convergence of the intrathalamic pathways that interconnect the TRN and VB (Huguenard and McCormick, 2007; Beenhakker and Huguenard, 2009). However, our knowledge of the functional organization of thalamic networks and its role in the spatiotemporal transformation of different types of afferent inputs remains incomplete.

We have shown previously that TRN neurons are the target of powerful cholinergic synaptic inputs (Sun et al., 2013). Here, by using an optogenetic approach, we find that brief activation of cholinergic afferents can trigger synchronous activation of TRN neurons, leading to persistent but asynchronous activity in thalamic networks. We identify several distinct circuit motives that underlie cholinergic-evoked thalamic network activity.

Materials and Methods

Thalamic slice preparation. Thalamic horizontal slices (400 μm) were obtained from both male and female bacterial artificial chromosome (BAC)-transgenic mice expressing channelrhodopsin-2 (ChR2) under the control of the choline acetyltransferase (ChAT) promoter (ChAT–ChR2–EYFP; Zhao et al., 2011), aged P13–P21. For experiments using wild-type mice, horizontal slices (400 μm) were obtained from C57BL/6 mice of either sex. Animals were anesthetized with isoflurane and decapitated following procedures in accordance with National Institutes of Health guidelines and approved by the University of Texas Health Science Center at Houston animal welfare committee. Slices were cut using a vibratome (Leica VT1200S) in an ice-cold sucrose-containing solution consisting of the following (in mM): 212 sucrose, 2.5 KCl, 1.25 NaH_2PO_4, 10 $MgSO_4$, 26 $NaHCO_3$, 11 glucose, and 0.5 $CaCl_2$ (saturated with 95% O_2–5% CO_2). Slices were incubated at 34°C for 50 min in saline solution containing the following (in mM): 126 NaCl, 26 $NaHCO_3$, 2.5 KCl, 1.25 NaH_2PO_4, 10 glucose, 2 $CaCl_2$, and 2 $MgCl_2$ (saturated with 95% O_2–5% CO_2). Slices were then kept at room temperature until used for experiments.

Electrophysiological recordings. Recordings were performed at 33–35°C using an in-line heater (Warner Instruments) while perfusing the recording chamber with saline solution, supplemented with glutamine (300 μM). We found that addition of glutamine enhanced the maintenance of network activity over multiple trials (Bryant et al., 2009) but had no influence on cell or network excitability. Visualized patch recordings were performed under infrared differential interference contrast visualization using an Olympus BX51WI microscope and an IR-1000 camera (Dage-MTI). Whole-cell voltage-clamp recordings from TRN and VB neurons were obtained using glass pipettes of 2–4 MΩ filled with an internal solution containing the following (in mM): 120 $CsMeSO_3$, 10 CsCl, 1 $MgCl_2$, 1 $CaCl_2$, 10 HEPES, 1 QX-314, 11 EGTA, 2 Mg-ATP, and 0.3 Na-GTP (adjusted to 295 mOsm and pH 7.3). Whole-cell current-clamp recordings from TRN neurons were obtained with an internal solution containing the following (in mM): 108 KGluc, 26 KCl, 2 $MgCl_2$, 0.16 $CaCl_2$, 10 HEPES, 0.5 EGTA, 2 Mg-ATP, and 0.4 Na-GTP (adjusted to 295 mOsm and pH 7.3). Loose-patch voltage-clamp or cell-attached

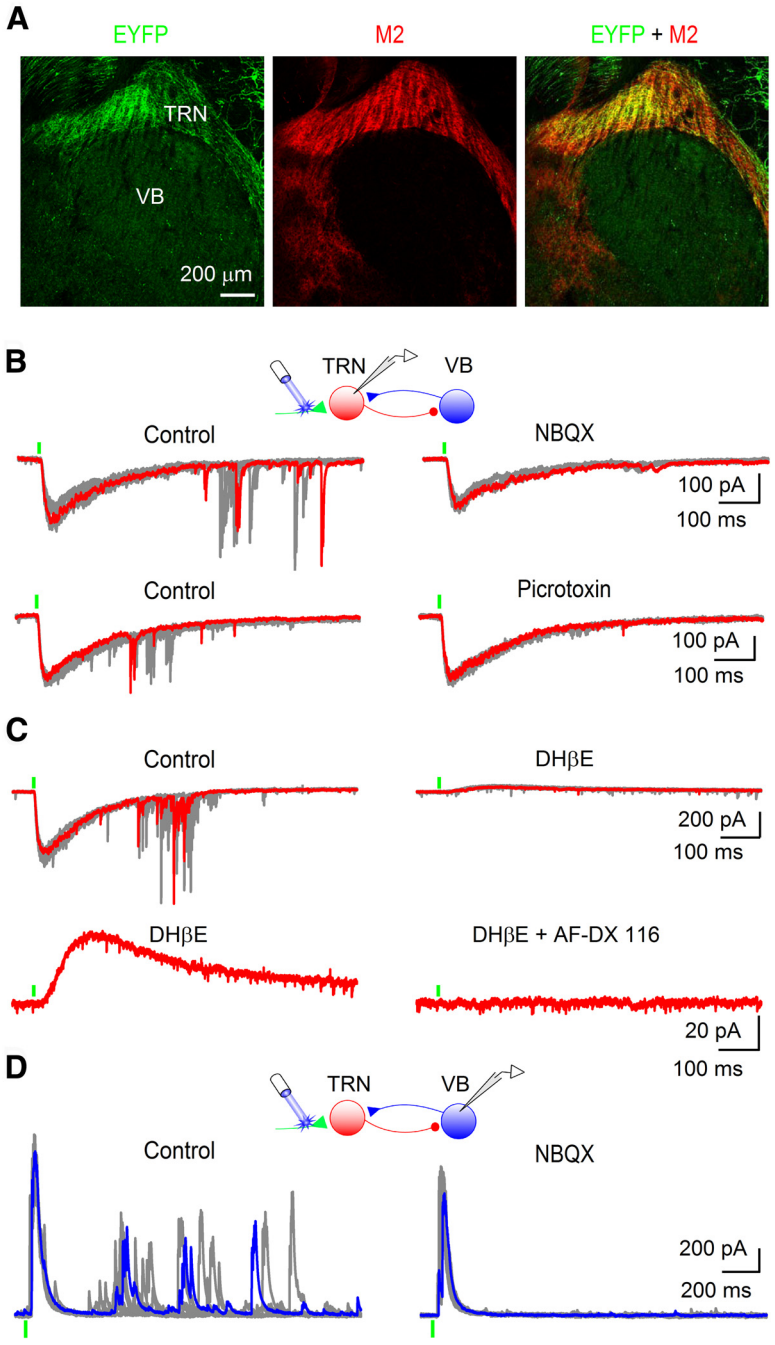

Figure 1. Cholinergic synaptic inputs trigger thalamic network activity. ***A***, Immunostaining for EYFP (left), M2 mAChRs (middle), and overlay (right) in coronal slices of ChAT–ChR2–EYFP BAC-transgenic mice. ***B***, Multiple consecutive trials showing that brief (0.3–1 ms) laser pulses trigger both short- and long-latency EPSCs in TRN neurons held in voltage clamp. Top, Long-latency EPSCs (recorded with a K-based internal solution) were reduced in amplitude by AMPAR antagonist (NBQX, 10 μM). Bottom, Glutamatergic EPSCs (recorded with a Cs-based internal solution) were eliminated by picrotoxin (50 μM). The schematic here and in the following figures indicate recording configuration. Green vertical bar indicates time of laser stimulation. ***C***, Top, Multiple consecutive trials showing that both short- and long-latency EPSCs (recorded with a K-based internal solution) were blocked by the nAChR antagonist DHβE (500 nM). Bottom, For the same TRN neuron, the remaining IPSC was blocked by the M2 mAChR antagonist AF-DX 116 (10 μM). Both traces are averages of eight individual trials. ***D***, Whole-cell voltage-clamp recordings from a VB neuron with Cs-based internal solution, held at 0 mV. Representative experiment showing multiple trials with oscillatory IPSCs evoked by single stimuli in TRN. Polysynaptic IPSCs were eliminated after bath application of NBQX (10 μM).

voltage-clamp and current-clamp recordings from TRN and VB neurons were obtained with pipettes (2–3 MΩ) filled with ACSF. For loose-patch recordings, the seal resistance was 50–100 MΩ, and, for cell-attached recordings, seal resistance was >1 GΩ. To minimize any influence on the cell membrane potential, holding voltage was adjusted continually to maintain a holding current near 0 pA (Perkins, 2006). For all experiments, cholinergic terminals were activated every 30 s with single laser pulses (0.3–1 ms) using a DL447 laser (Crystalaser) at a wavelength of 440–447 nm. The laser was focused to a ~20 μm diameter spot through a 60× water-immersion objective. Maximal total laser power at the focal plane was 10 mW. Extracellular electrical stimuli (10–60 μA) were applied with pipettes pulled from theta glass (10–15 μm tip diameter; WPI) and filled with saline solution.

Previous work has shown that ChAT–ChR2–EYFP BAC-transgenic mice carry additional copies of the vesicular ACh transporter gene (Kolisnyk et al., 2013), which could potentially alter the synaptic release of ACh. However, under our experimental conditions, we found that the properties of cholinergic signaling in the TRN (threshold EPSC amplitude values, biphasic responses, and short-term synaptic plasticity) were comparable between BAC-transgenic mice and wild-type animals, justifying the use of this model system.

NBQX, dihydro-β-erythroidine hydrobromide (DHβE), 11-[[2-[(diethylamino)methyl]-1-piperidinyl]acetyl]-5,11-dihydro-6H-pyrido[2,3-b][1,4]benzodiazepin-6-one (AF-DX 116) picrotoxin, (2S)-3-[[(1S)-1-(3,4-dichlorophenyl)ethyl]amino-2-hydroxypropyl](phenylmethyl)phosphinic acid (CGP 55845) D-APV, and apamin were obtained from R&D Systems. All other chemicals were obtained from Sigma-Aldrich.

Data acquisition and analysis. Recordings were acquired using a Multiclamp 700B amplifier (Molecular Devices), filtered at 2–10 kHz, and digitized at 20 kHz with a 16-bit analog-to-digital converter (Digidata 1440A; Molecular Devices). Data were acquired using Clampex 10.3 software (Molecular Devices) and analyzed using custom macros written in Igor Pro (Wavemetrics). Synchronous synaptic inputs were determined by calculating a synchrony index, defined as the ratio of the synaptic events that occurred in both cells within a 5 ms window to the total number of events. Pearson's correlation coefficient was calculated using the following equation:

Peason's Coefficient

$$= \frac{\sum_{i=0}^{n-1}(\text{Cell A}[i] - \overline{\text{Cell A}})(\text{Cell B}[i] - \overline{\text{Cell B}})}{\sqrt{\sum_{i=0}^{n-1}(\text{Cell A}[i] - \overline{\text{Cell A}})^2 \sum_{i=0}^{n-1}(\text{Cell B}[i] - \overline{\text{Cell B}})^2}},$$

where Cell A denotes the signal in the reference neuron, and Cell B denotes the signal of target neuron. To calculate cross-correlations of postsynaptic responses, recordings were bandpass filtered (1.5–70 Hz) before performing shift-corrected cross-correlations. For APs recorded in pairs of neurons, activity was binned into 5 ms windows to obtain AP trains for each neuron. Shift-corrected cross-correlation was performed in Igor Pro (Wavemetrics) using the following equation:

$$\text{CC}[\text{lag}] = \sum_{i=0}^{n-1} \text{Cell A}[i] \times \text{Cell B}[\text{lag} + i],$$

where Cell A denotes the signal in the reference neuron, and Cell B denotes the signal of target neuron. Statistical analyses were performed using paired or unpaired Student's *t* tests. Differences were considered statistically significant at $p < 0.05$. Data are presented as mean ± SEM unless otherwise indicated.

Immunohistochemistry. Immunohistochemical staining was performed as described previously (Wu et al., 2010). Brains were sectioned coronally or sagittally into 50-μm-thick sections with a Leica VT1000S vibrating microtome. Sections were counterstained with DAPI and mounted with Vectashield (Vector Laboratories). Three primary antibodies, rat anti-M2 mAChR (1:1000; Millipore), chicken anti-GFP (1:1000; Aves Labs), and goat anti-ChAT (1:200; Millipore), were used. Fluorescent signals for M2 mAChRs and EYFP were detected by using the secondary antibodies goat anti-rat Alexa Fluor 594 (1:1000; Invitrogen) and goat anti-chicken IgG–Alexa Fluor 488 (1:1000; Invitrogen), respectively. Fluorescent signals for ChAT and EYFP were detected by using the secondary antibodies donkey anti-goat IgG–Alexa Fluor 647 (1:1000; Invitrogen) and donkey anti-chicken IgG–Alexa Fluor 488 (1:1000; Invitrogen), respectively. Fluorescent images were obtained using a Zeiss 710 confocal microscope.

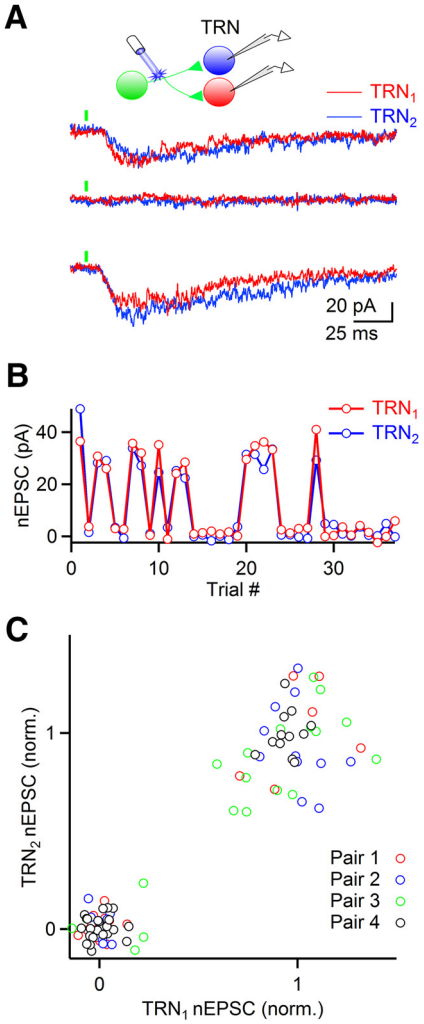

Figure 2. Single cholinergic axons form synapses onto neighboring TRN neurons. ***A***, Voltage-clamp recordings from two adjacent TRN neurons, showing nEPSCs and response failures in consecutive trials. Cells were recorded with a Cs-based internal solution. ***B***, For the two cells shown in ***A***, the graph indicates covariation of successes and failures of nEPSCs, indicating that recorded neurons received divergent input from single cholinergic axons. ***C***, Summary plotting response failures and successes, with amplitude values for a given neuron normalized by the average of all successful trials ($n = 4$ TRN cell pairs).

Results

Activation of cholinergic synaptic inputs to the TRN generates thalamic network activity

Cholinergic afferents form extensive synaptic connections with TRN neurons, but their role in controlling thalamic network activity is poorly understood. To address this question, we performed experiments using whole-cell and cell-attached recordings in horizontal thalamic slices of ChAT–ChR2–EYFP BAC-transgenic mice that express ChR2 specifically in cholinergic neurons (Zhao et al., 2011). Immunostaining revealed strong EYFP expression in the TRN, whereas expression was very low in the adjacent VB (Fig. 1*A*). We found that single laser stimuli (0.3–1 ms, 1–10 mW) directed to the TRN led to short-

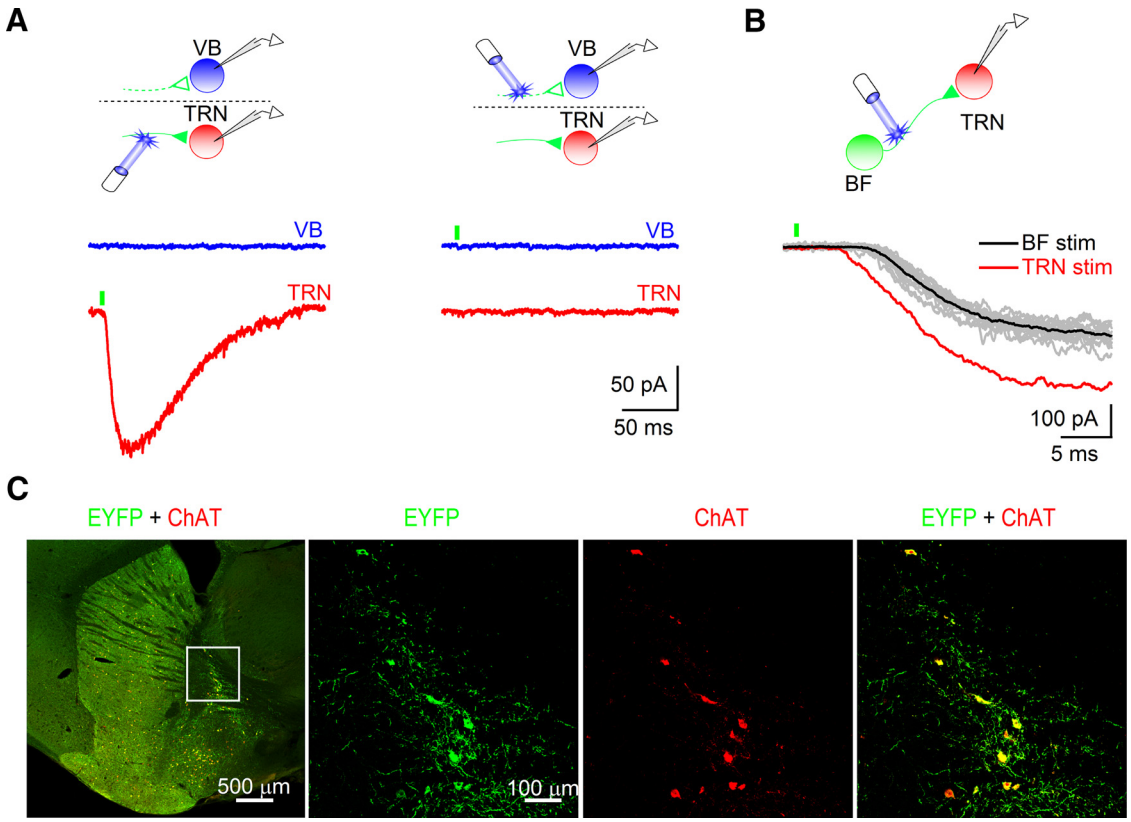

Figure 3. Activation of BF cholinergic afferents triggers synaptic responses in TRN neurons. ***A***, Representative recordings from a TRN–VB neuronal pair using K-based internal solution. Fast glutamatergic and GABAergic synaptic transmission was blocked pharmacologically. Laser stimuli were placed either in the TRN (left) or VB (right), near the recorded cell. Cholinergic responses were only detected in TRN neurons after local stimulation. Responses shown are averages of five consecutive trials. ***B***, Representative recording from a TRN neuron using a Cs-based internal solution in a sagittal brain slice, showing that placing laser stimulation into the BF region (black trace) generated monosynaptic nEPSCs with slightly longer latencies compared with nEPSCs evoked by local stimulation (red trace). EPSCs shown are averages of 15 consecutive trials. Individual trials (gray traces) indicate minimal latency jitter for BF-evoked nEPSCs. ***C***, Immunohistochemical staining for EYFP–ChR2 and ChAT in the BF of ChAT–ChR2–EYFP BAC-transgenic mice. Expression of EYFP–ChR2 was detected by green fluorescence. ChAT expression was detected by antibodies against ChAT (red). Left, Overlay of ChAT and EYFP at low magnification (green and red). Right, Higher-magnification views for the BF area indicated in the left.

latency nicotinic EPSCs (nEPSCs) in all cells examined (Fig. 1*B*; latency, 4.1 ± 0.2 ms; amplitude, 350.2 ± 39.8 pA; rise time, 15.5 ± 1.8 ms; $n = 32$ cells). Our previous study demonstrated that large-amplitude nEPSCs are generated by the simultaneous activation of a small number of individual axons (>10) converging onto a given neuron (Sun et al., 2013). To test whether individual cholinergic axons can form diverging contacts with multiple TRN neurons, we performed dual recordings from neighboring TRN neurons (<50 μm intersomatic distance) and activated individual cholinergic axons at a minimal laser intensity generating both nEPSCs and failures (Fig. 2*A*,*B*). For the cell pairs examined, we could isolate threshold responses, for which successes and failures occurred in common trials (Fig. 2*C*; $n = 4$), indicating that both neurons were activated by the same presynaptic axon. Thus, cholinergic afferents to TRN neurons are characterized by both axonal divergence and convergence.

In the majority of recordings (24 of 32 cells), laser stimuli led to multiple additional EPSCs (latency, 278.3 ± 12.7 ms; duration of activity, 524.3 ± 46.0 ms; number of EPSCs/trial, 15.7 ± 1.5; $n = 24$ cells), characterized by large amplitudes and fast kinetics (amplitude, 366.5 ± 66.4 pA; rise time, 0.20 ± 0.01 ms; $n = 24$ cells), with considerable jitter from trial to trial (Fig. 1*B*). Bath application of the AMPA receptor (AMPAR) antagonist NBQX strongly reduced the amplitude of the long-latency synaptic responses (Fig. 1*B*; control, 299.1 ± 89.9 pA; NBQX, 18.4 ± 1.5 pA; $n = 5$ cells), indicating that they are generated by glutamatergic synapses. In addition, the nAChR antagonist DHβE (500 nM) blocked nEPSCs and completely eliminated glutamatergic EPSCs (Fig. 1*C*; control, 15.2 ± 2.9 EPSCs per trial; DhβE, 0 ± 0 EPSCs per trial; $n = 5$), indicating that nAChR activation was required for the generation of long-latency responses. The presence of DHβE revealed a slow muscarinic IPSC (latency, 33.0 ± 2.8 ms; amplitude, 35.3 ± 6.7 pA; rise time, 87.7 ± 17.3 ms; $n = 5$ cells) that was blocked by the M2 mAChR antagonist AF-DX 116. Thus, release of ACh triggered by single laser pulses can lead to biphasic postsynaptic responses in TRN neurons, in agreement with our findings using electrical stimulation (Sun et al., 2013) and, in addition, to the generation of glutamatergic responses.

We next determined the mechanisms underlying cholinergic-evoked network activity. Thalamic circuits are organized as reciprocal loops, in which inhibitory inputs from TRN neurons can generate rebound bursting in thalamic cells, in turn leading to re-excitation of TRN neurons (Huguenard and McCormick, 2007). If cholinergic inputs evoke thalamic activity via rebound firing in VB neurons, blocking GABAergic synaptic transmission should eliminate glutamatergic responses recorded in TRN neurons. In agreement, we found that bath application of picrotoxin completely eliminated glutamatergic EPSCs (Fig. 1*B*; control, 15.3 ± 4.0 EPSCs per trial; picrotoxin, 0.1 ± 0.0 EPSCs per trial; $n = 5$ cells), whereas the $GABA_BR$ antagonist CGP 55845 had little effect on thalamic network activity (control, 9.9 ± 1.8

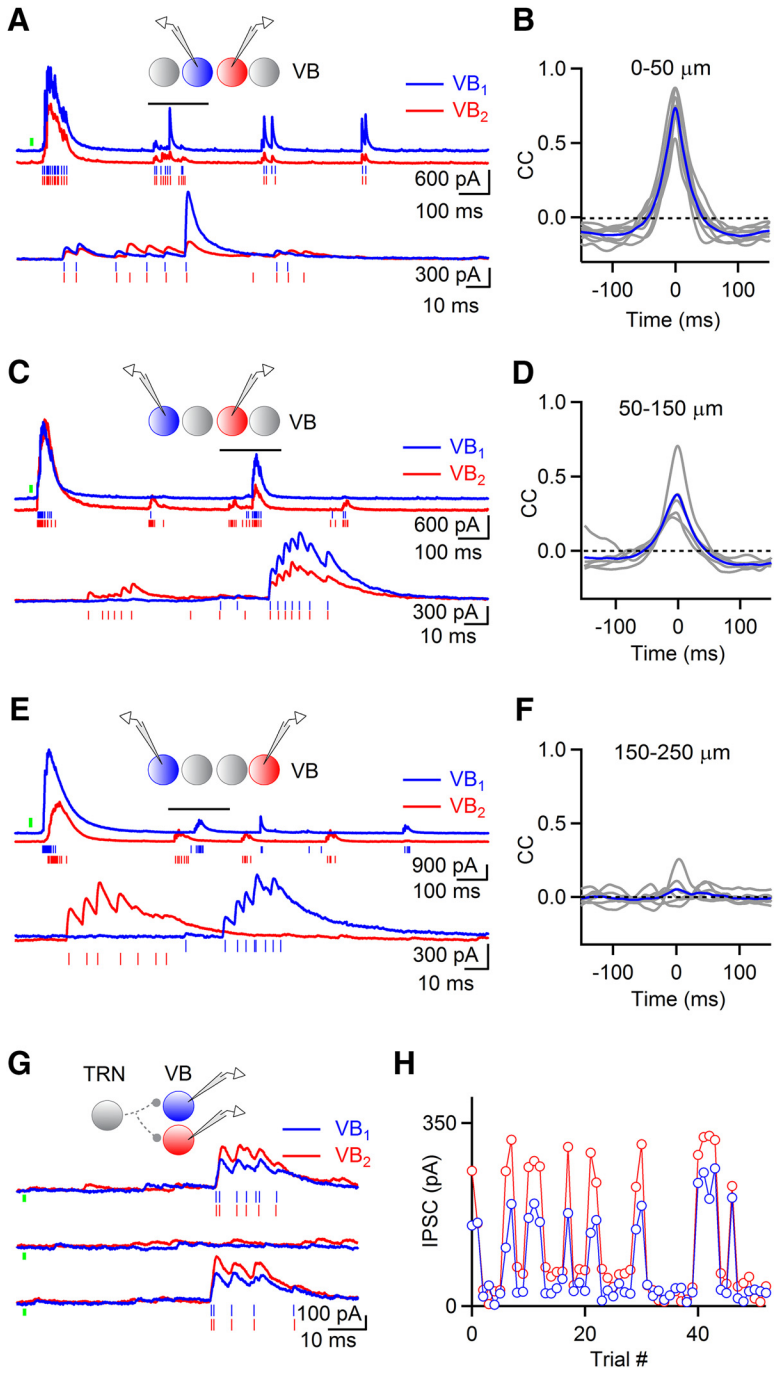

Figure 4. Local clusters of VB neurons receive shared synaptic input from the TRN. ***A–F***, Dual voltage-clamp recordings from pairs of VB neurons at different intersomatic distances. Cells were recorded with a Cs-based internal solution and held at 0 mV. Representative recordings show synchronous IPSCs for neighboring VB neurons (20 μm distance) in response to laser stimulation (***A***), partially synchronous IPSCs for neurons at an intermediate distance (90 μm, ***C***), and non-synchronous IPSCs for neurons at a large distance (190 μm, ***E***). Vertical bars (red and blue) denote IPSC onsets. Traces at the bottom show close-ups for the time period indicated by the horizontal bar in the traces above. Cross-correlograms of polysynaptic IPSC activity (200–1500 ms) in cell pairs at close (***B***, 0–50 μm, $n = 9$), intermediate (***D***, 50–150 μm, $n = 5$), and large (***F***, 150–250 μm, $n = 8$) intersomatic distance pairs, with average shown in blue. ***G***, ***H***, Divergent synaptic contacts formed by individual TRN neurons onto neighboring thalamic neurons. Laser intensity was adjusted to evoke disynaptic IPSC in ~50% of all trials. ***G***, Voltage-clamp recordings show common IPSCs and response failures in consecutive trials. Vertical bars (red and blue) denote onset of individual IPSCs in the two cells. ***H***, For the same pair, the graph plots IPSC amplitudes for both neurons in consecutive trials.

EPSCs per trial; CGP 55845, 9.4 ± 1.9 EPSCs per trial; $n = 5$ cells). Next, we recorded cholinergic-evoked synaptic activity in VB neurons, whose only source of inhibition originates in TRN. Single laser pulses triggered rhythmic IPSCs (Fig. 1*D*) at a frequency of 3.9 ± 0.2 Hz that lasted 1.3 ± 0.1 s and had an average of 4.8 ± 0.4 events ($n = 31$ cells). Initial, short-latency IPSCs had little latency jitter from trial to trial (latency, 29.7 ± 1.5 ms; SD, 2.7 ± 0.3, $n = 31$ cells), suggesting that they were disynaptic and generated by TRN neurons that were monosynaptically activated by cholinergic inputs. In contrast, long-latency IPSCs had considerable jitter from trial to trial, suggesting that they were mediated by TRN neuronal firing evoked by glutamatergic thalamoreticular inputs. In agreement, NBQX completely blocked long-latency IPSCs (Fig. 1*D*; control, 3.0 ± 0.8 long-latency events per trial; NBQX, 0.1 ± 0.0 long-latency events per trial; $n = 6$ cells) but had no influence on short-latency IPSCs. Together, these data show that the activation of cholinergic inputs with single stimuli can trigger robust oscillatory responses in thalamic networks.

Cholinergic responses in TRN are evoked by inputs from the BF

We next determined whether fast cholinergic signaling in the thalamus is nucleus specific by performing simultaneous recordings from TRN–VB neuronal pairs in the presence of receptor antagonists for glutamatergic and GABAergic synaptic transmission. Laser stimuli were directed to either TRN or VB, near the recorded neuron. Although laser stimuli in TRN evoked large-amplitude nEPSCs in all TRN neurons, no postsynaptic responses could be detected in VB after laser stimulation in the VB or TRN (Fig. 3*A*; $n = 6$ pairs). Identical results were obtained using extracellular stimulation in slices obtained from wild-type animals ($n = 3$ TRN–VB pairs; data not shown). Thus, under our experimental conditions, short-latency cholinergic signaling is restricted to the TRN.

Previous anatomical studies have suggested that cholinergic neurons in the BF target TRN but not adjacent sensory thalamic nuclei (Hallanger et al., 1987; Levey et al., 1987). As described previously (Zhao et al., 2011), we found that, in ChAT–ChR2–EYFP mice, virtually all ChAT-positive neurons in the BF also showed strong expression of ChR2–EYFP (Fig. 3*C*; ratio of EYFP/ChAT, 0.96). To obtain independent evidence for the activation of TRN neurons by BF cholinergic inputs, we prepared sagittal slices to preserve synaptic connections between the BF and TRN. We found that BF laser stimulation reliably evoked monosynaptic responses in the TRN with minimal latency jitter, at longer latencies compared with local TRN stimulation

(Fig. 3*B*; BF-evoked response latency, 7.3 ± 0.4 ms, $n = 7$ cells; TRN-evoked response latency, 4.1 ± 0.2 ms, $n = 24$ cells; $p < 0.001$). These data indicate that BF cholinergic neurons can generate reliable short-latency synaptic responses in TRN neurons.

Local clusters of VB neurons receive shared inputs from the TRN

Previous studies performed *in vivo* and *in vitro* have led to the suggestion that intrathalamic oscillatory activity evoked by glutamatergic inputs is accompanied by synchronous firing in thalamic networks, in part mediated by extensive synaptic convergence and divergence between TRN and thalamic neurons and by electrical coupling within the TRN (Huguenard and McCormick, 2007; Beenhakker and Huguenard, 2009). We tested whether VB neurons receive common inhibitory inputs from TRN cells by recording laser-evoked rhythmic IPSCs from pairs of VB neurons. For neighboring neurons (<50 μm intersomatic distance), both the disynaptic IPSC and long-latency polysynaptic IPSCs (Fig. 4*A*) were highly synchronous. Analysis of individual IPSCs showed that their onset times were identical for pairs of neighboring VB neurons (synchrony index, 0.81 ± 0.01; $n = 9$ pairs). Moreover, cross-correlograms of the polysynaptic IPSCs revealed synchronous fluctuations in membrane currents (Fig. 4*B*; Pearson's correlation coefficient, 0.73 ± 0.03; $n = 9$ pairs). IPSC synchrony was strongly dependent on the intersomatic distance of VB neuronal recordings. For dual recordings ranging from 50 to 150 μm intersomatic distance in which both cells showed rhythmic IPSCs (Fig. 4*C*,*D*), some synaptic events occurred simultaneously in both neurons, whereas others were limited to a single cell (synchrony index, 0.2 ± 0.05; Pearson's correlation coefficient, 0.37 ± 0.08; $n = 5$ pairs). In recordings from pairs at distances ranging from 150 to 250 μm (Fig. 4*E*,*F*), polysynaptic IPSCs were completely independent (synchrony index, 0.05 ± 0.01; Pearson's correlation coefficient, 0.05 ± 0.003; $n = 8$ pairs). These data indicate the local VB neurons share inhibitory input from a common group of presynaptic TRN neurons, whereas for neurons at distances larger than 150 μm, afferent inhibition is generated by independent clusters of TRN neurons. To further confirm that individual TRN neurons form divergent synaptic connections with local VB cells, we recorded threshold IPSCs (~50% response failures) in pairs of VB neurons located within 50 μm (Fig. 4*G*,*H*). For all cell pairs ($n = 5$), response failures and successes were synchronous for the two recordings. Furthermore, for trials generating IPSCs, IPSC latency and the number and onset of individual synaptic events were identical for simultaneously recorded neurons. Thus, neighboring VB neurons are the target of shared inhibitory inputs, likely generated by TRN neurons with extensive local axonal arborizations.

BF-evoked VB neuronal activity is asynchronous

Does the presence of shared inhibitory inputs lead to synchronous rebound burst firing in neighboring VB neurons? To address this question, we recorded laser-evoked AP activity from pairs of neighboring VB neurons in cell-attached mode to avoid perturbations in intracellular chloride concentration (Fig. 5*A*). As described above, single laser pulses led to highly reliable and synchronous disynaptic inhibitory responses in the two neurons recorded. In contrast, rebound Ca^{2+} spikes (recorded in current clamp) and fast Na^{+}-dependent APs (recorded in voltage clamp) showed considerable fluctuations from trial to trial (Fig. 5*A*–*C*; latency of initial APs, 418.6 ± 27.3 ms; SD, 94.8 ± 14.5; $n = 25$). In addition, latency differences for the initial AP were large between neighboring neurons (Fig. 5*D*; 180.6 ± 43.2 ms; $n = 10$ cell pairs) and fluctuated strongly from trial to trial (SD, 127.3 ± 32.6; $n = 10$ pairs).

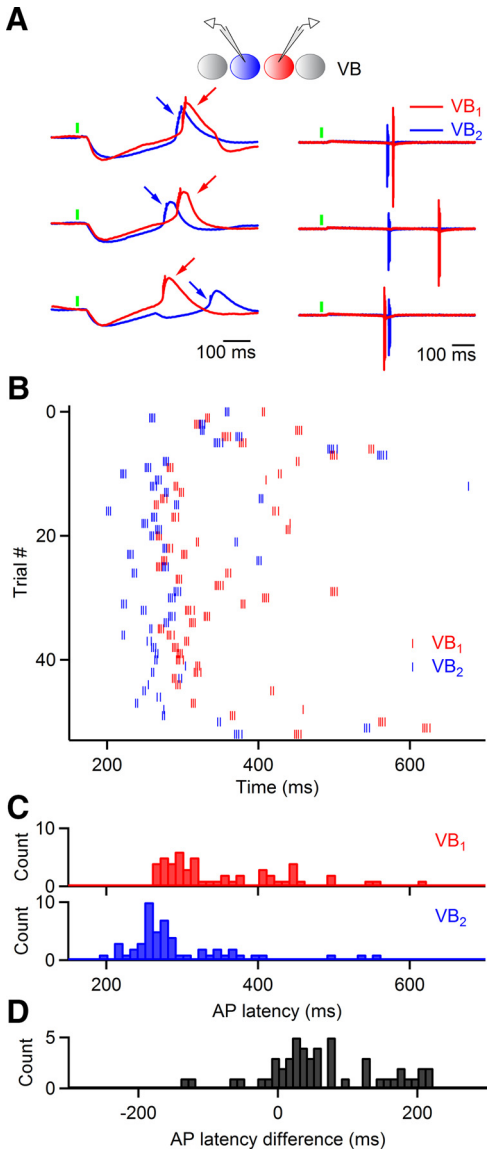

Figure 5. Cholinergic inputs evoke asynchronous firing in neighboring thalamic neurons. ***A***, Simultaneous cell-attached recordings from neighboring VB neurons, held in either current clamp (left) or voltage clamp (right) showing synchronous and precise disynaptic inhibition (left) but imprecise and asynchronous AP firing (right). Rebound Ca^{2+} spikes are indicated by arrows (left). Three consecutive trials are shown for each recording configuration. ***B***, Raster plot shows AP activity in a VB neuronal pair recorded in cell-attached mode, evoked by cholinergic stimulation at $t = 0$ ms. ***C***, Distribution of initial AP latency evoked by cholinergic stimulation in the two neurons. Bin size, 5 ms. Latency for VB_1 is 356.4 ± 86.5 ms and for VB_2 is 295.1 ± 75.0 ms (mean ± SD). ***D***, The graph plots the distribution of the initial AP latency difference ($VB_1 - VB_2$). Bin size, 5 ms. Latency difference, 63.2 ± 83.4 ms (mean ± SD). Data in ***B–D*** are from the same pair.

Previous work has shown that both probability and latency of thalamic rebound bursting depend on IPSP amplitude and kinetics, as well as cell-specific differences in postsynaptic conductances (Sohal et al., 2006), which could at least partly explain the large differences in AP timing for neighboring neurons. In addition, local network activity might contribute to AP jitter for a given neuron and further desynchronize activity between neurons; under this scenario, VB neurons firing at short latencies could rapidly recruit TRN neurons, whose activity then delays AP

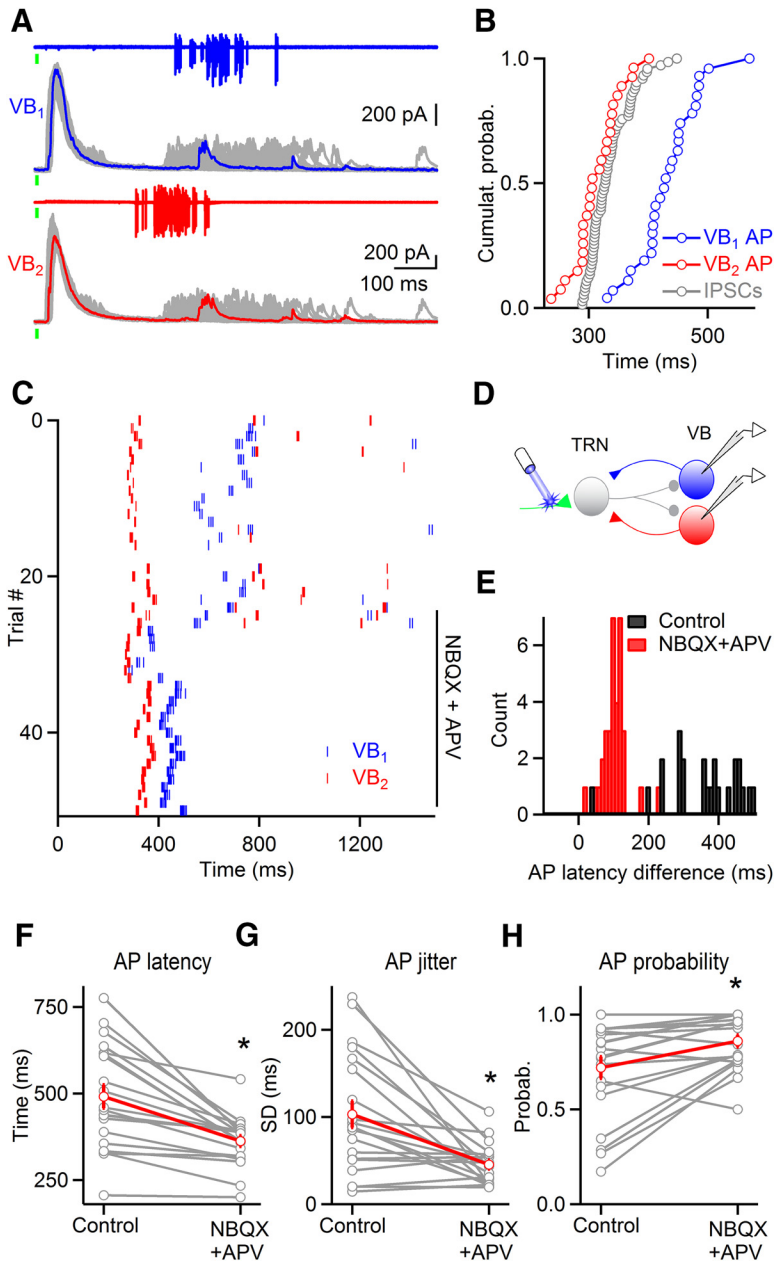

Figure 6. TRN-mediated lateral inhibition desynchronizes thalamic activity. ***A***, VB neuronal firing can temporally overlap with polysynaptic inhibition. Dual cell-attached recording from neighboring VB neurons showing AP timing followed by whole-cell voltage clamp to record IPSCs for the same pair. ***B***, Cumulative probability of initial AP latency and time of onset of polysynaptic IPSCs for the neurons shown in ***A***, evoked by cholinergic stimulation at $t = 0$ ms. ***C***, Raster plot shows cholinergic-evoked AP activity in a pair of neighboring VB neurons before and during application of NBQX (10 μM) and APV (25 μM). ***D***, Schematic depicting circuit mediating lateral inhibition. ***E***, The graph plots distribution of initial AP latency difference ($VB_2 - VB_1$) before (black) and during (red) application of NBQX and APV. Bin size, 10 ms. ***F–H***, Summary data plotting change in the latency of initial AP (***F***), in the jitter of the initial AP (***G***), and in the probability of cholinergic-evoked VB firing (***H***), after bath application of NBQX and APV. Red traces depict average ± SEM. *$p < 0.01$, paired t test, $n = 20$ VB neurons.

timing in neighboring VB neuron, via a process termed open-loop or lateral inhibition (Fig. 6*D*), as postulated previously (Pinault, 2004). To examine this possibility, we recorded from neurons in cell-attached mode to determine AP timing, before establishing whole-cell mode to record IPSCs in voltage clamp. We found that, in some neurons, polysynaptic IPSCs occurred before AP generation (Fig. 6*A*,*B*), suggesting that they could be involved in delaying AP initiation. To directly determine the influence of lateral inhibition in AP timing, we recorded from single or pairs of thalamic neurons in cell-attached mode, before eliminating polysynaptic inhibition with NBQX and APV. Across all neurons examined, blocking polysynaptic inhibition led to a significant reduction in both AP latency (Fig. 6*C*,*F*; control, 491.1 ± 33.6 ms; NBQX + APV, 361.9 ± 15.9 ms; $n = 20$ cells) and AP jitter (Fig. 6*C*,*G*; control, 102.8 ± 15.3; NBQX + APV, 45.3 ± 5.1; $n = 20$) and, in addition, to an increase in AP probability (Fig. 6*H*; control, 0.72 ± 0.06; NBQX + APV, 0.86 ± 0.03; $n = 20$). For pairs of VB neurons, this led to a reduction of both mean AP latency difference (control, 233.6 ± 51.8 ms; NBQX + APV, 100.5 ± 35.7 ms; $n = 6$ cell pairs) and its trial-to-trial fluctuation (control, 157.9 ± 49.6; NBQX + APV, 48.9 ± 14.7; $n = 6$ cell pairs), as shown for a representative experiment (Fig. 6*E*). Notably, even in the absence of lateral inhibition, trial-to-trial fluctuations in initial AP timing remained considerably larger compared with the latency jitter of the underlying disynaptic IPSC (45.3 ± 5.1 for APs, $n = 20$; 2.7 ± 0.3 for IPSC, $n = 31$), indicating that synaptically evoked rebound bursting in VB neurons is imprecise. Together, these data suggest that cholinergic-evoked feedforward inhibition and TRN-mediated lateral inhibition interact to generate asynchronous firing of local VB neurons.

A low divergence of thalamoreticular connections underlies asynchronous TRN neuronal activity

Although AP output in VB neurons displayed little synchrony during cholinergic-evoked activity, synchronous firing might be more pronounced in networks of TRN neurons, thereby playing an important role in sustaining thalamic activity. Individual thalamic inputs can form powerful connections with TRN neurons (Gentet and Ulrich, 2003), predicting that even a moderate degree of thalamoreticular synaptic divergence could generate synchronous excitation and AP firing in local populations of TRN neurons. To measure TRN neuronal firing during BF evoked activity, we performed cell-attached and whole-cell recordings from pairs of closely spaced TRN neurons (Fig. 7). Single laser stimuli led to reliable, short-latency burst firing in individual TRN neurons (latency, 26.3 ± 1.3 ms; jitter, 2.1 ± 0.19 ms; APs per burst, 4.0 ± 0.2; $n = 52$ cells), as shown previously (Sun et al., 2013). For some neurons, initial burst firing was followed by additional APs at longer latencies. In pairs of neighboring TRN neurons (<50 μm distance) for which both cells generated short-latency bursts and at least one neuron generated additional persistent activity, only 4 of 24 pairs showed such activity in both neurons, and this activity was never synchronized. Instead, for

the large majority of pairs, persistent AP firing could only be detected in a single neuron (Fig. 7*A*), indicating that thalamoreticular connections triggering suprathreshold activity are sparse. For cell pairs recorded in whole-cell mode in which at least one neuron generated glutamatergic EPSCs, 25 of 30 pairs displayed such activity in both cells (Fig. 7*C*). Surprisingly, glutamatergic synaptic inputs were rarely synchronized for neighboring neurons (Fig. 7*C–E*), even if individual EPSPs in a given cell were large enough to trigger APs (Fig. 7*B*). To verify that neighboring TRN neurons had at least a moderate degree of dendritic overlap that should enhance the likelihood of shared excitatory input from individual thalamic neurons, we performed recordings from pairs of electrically coupled TRN neurons. However, glutamatergic EPSCs showed very little synchrony, indistinguishable from pairs without electrical coupling (Fig. 7*D*,*E*; peak cross-correlation (CC) for electrically coupled neurons, 0.109 ± 0.038, $n = 5$ pairs; peak CC for non-coupled neuronal pairs, 0.110 ± 0.039, $n = 14$ pairs), indicating that the synaptic divergence of individual thalamic neurons is minimal in TRN.

It is possible that the synaptic connectivity between TRN and VB is artificially low in our slice preparation, explaining the lack of synchronous firing among neighboring neurons. To address this concern, we performed experiments in the presence of the SK channel blocker apamin, to prolong burst firing in TRN neurons. As a result, TRN-mediated inhibition in VB neurons should be enhanced, thereby recruiting additional VB neurons to generate rebound bursts, ultimately generating more robust rhythmic activity. In agreement, we found that apamin led to a significant prolongation in nEPSP-evoked burst firing in TRN neurons (Fig. 8*A*; control, 4.1 ± 0.3 spikes per burst; apamin, 15.8 ± 1.2 spikes per burst; $n = 10$ cells) and a dramatic increase in the duration of rhythmic activity, for TRN (Fig. 8*A–C*) and VB (Fig. 8*E*,*F*) neurons (TRN, 3.4 ± 0.4 s, $n = 10$ cells; VB, 3.0 ± 0.5 s; $n = 8$ cells). However, even under these conditions, neuronal pairs in TRN ($n = 5$) or VB ($n = 4$) did not generate synchronous APs (Fig. 8*D*,*G*), and subthreshold activity for pairs of TRN neurons remained asynchronous (Fig. 8*D*).

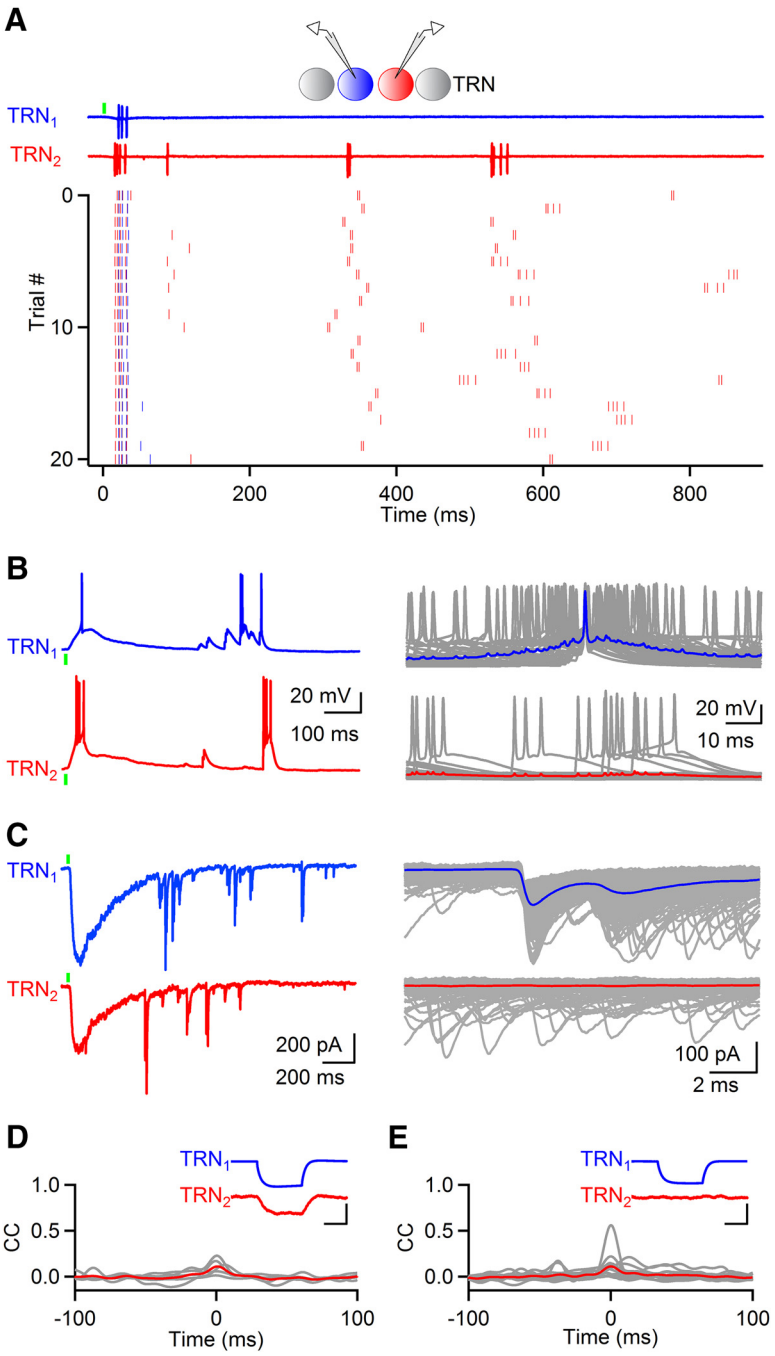

Figure 7. Adjacent TRN neurons receive powerful but independent thalamic inputs. ***A***, Top, Dual cell-attached recordings from neighboring TRN neurons show laser-evoked AP activity. Bottom, Raster plot showing APs for the same neuronal pair. ***B***, Left, Dual whole-cell current-clamp recordings from neighboring TRN neurons during laser-evoked network activity. Right, Recordings in TRN_2 temporally aligned with VB-evoked AP activity in TRN_1. Averages of all aligned recordings are shown in color. ***C***, Left, Whole-cell voltage-clamp recordings from the same pair of TRN neurons shown in ***B***. Right, Recordings in TRN_2 temporally aligned with VB-evoked EPSCs in TRN_1. Averages of all aligned recordings are shown in color. ***D***, ***E***, Cross-correlograms of glutamatergic EPSCs in pairs of electrically coupled (***D***, $n = 5$) or non-coupled (***E***, $n = 14$) TRN neurons, with the average shown in red. Insets show representative dual recordings, with hyperpolarizing current step (−100 pA) applied to TRN_1. Calibration: Scale bar: TRN_1, 20 mV, 50 ms; TRN_2, 0.8 mV, 50 ms.

Discussion

Here we provide the first functional demonstration for a BF cholinergic projection to TRN, leading to synchronous GABAergic activity in local clusters of thalamic VB neurons. BF cholinergic control of sensory processing can thus occur on both cortical and subcortical levels, as was proposed previously (Thiele, 2009; Pinto et al., 2013). A unique aspect of the thalamic circuit under study is the presence of three distinct transmitter systems, each of which is uniquely involved in generating network activity. This has allowed us to trace the flow of activity over four relays and has

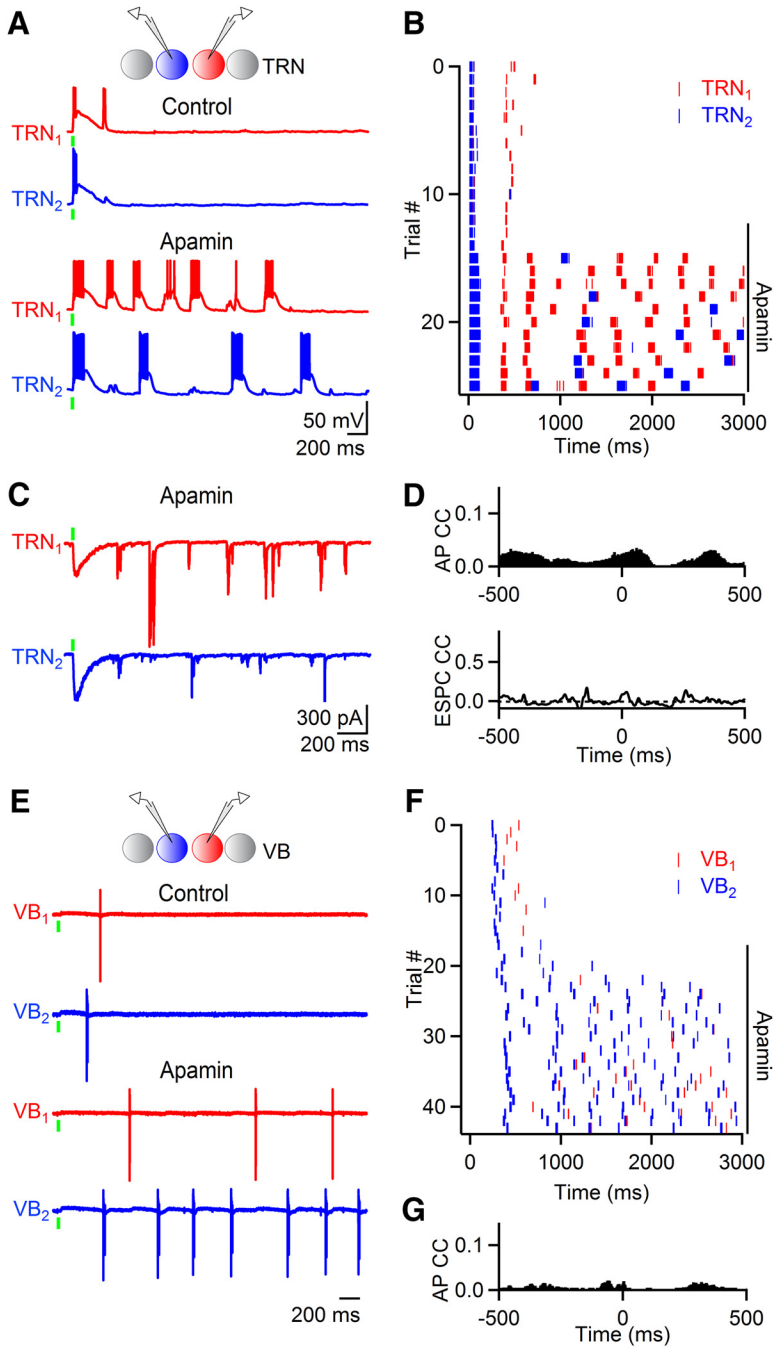

Figure 8. Enhancing oscillatory activity in thalamic networks does not lead to synchronous firing. ***A***, Cholinergic-evoked activity in a pair of neighboring TRN neurons before and after bath application of apamin (100 nM). To enhance visualization of individual spikes, only 3 s of activity are shown here and in the recordings below. ***B***, Raster plot shows cholinergic-evoked AP activity for the same pair over multiple trials, before and after application of apamin. Cholinergic inputs were activated at $t = 0$ ms, every 45 s. ***C***, Representative recordings of EPSCs after bath application of apamin, for the same pair shown in ***A***. ***D***, Cross-correlograms of AP activity (top) and glutamatergic synaptic activity (bottom) during apamin application for the same pair. ***E***, Cell-attached recordings from a pair of neighboring VB neurons before and after bath application of apamin. ***F***, Raster plot shows AP activity for the same pair over multiple trials, before and during application of apamin. Cholinergic inputs were activated at $t = 0$ ms, every 45 s. ***G***, Cross-correlogram of AP activity during bath application of apamin.

led to the identification of a number of thalamic circuit motives, namely highly divergent and convergent reticulothalamic connectivity, lateral inhibition, and sparse but powerful thalamoreticular connectivity. We propose that these circuit features are critical in preventing thalamic networks from generating synchronous activity under a variety of physiological conditions (Fig. 9).

BF cholinergic pathway targets the TRN

We found that optical activation of cholinergic neurons in the BF leads to strong postsynaptic responses specifically in TRN neurons. This confirms anatomical studies suggesting that BF cholinergic projections only innervate the TRN but avoid sensory and motor nuclei in the dorsal thalamus (Hallanger et al., 1987; Levey et al., 1987). As of now, anatomical studies that characterize the complete axonal tree of BF neurons do not exist, so it is unknown whether BF cholinergic projections to the TRN are formed by the same neurons that send afferents into the neocortex.

Our previous work has shown that the convergence of a small number of cholinergic afferents is sufficient to trigger APs in TRN neurons, because nEPSPs are amplified by the activation of T-type Ca^{2+} channels in distal dendrites (Sun et al., 2013). Here, we extend these findings by demonstrating that individual cholinergic axons can contact multiple TRN neurons. Thus, activity in a small number of BF cholinergic neurons is able to recruit clusters of neighboring TRN neurons. Whether electrical synapses formed by local TRN neurons (Long et al., 2004) play a role in synchronizing BF-evoked neuronal firing remains to be determined.

Under our experimental conditions, we could not detect cholinergic synaptic responses in VB neurons after local optical or electrical stimulation. Similarly, we could not evoke responses in TRN by potentially activating brainstem cholinergic fibers using stimulating electrodes or laser stimulation located in VB. Laser-evoked activation of brainstem cholinergic afferents might have been weak because of a low expression of ChR2 in ChAT–ChR2 mice. Furthermore, slicing could have damaged cholinergic axons from the brainstem although BF cholinergic afferents remain functional. Alternatively, it is possible that cholinergic signaling in the dorsal thalamus is mediated by distinct synaptic structures and requires specific conditions leading to significant ACh release and activation of postsynaptic targets. Understanding the synaptic mechanisms of how cholinergic afferents from the brainstem influence information processing in thalamic circuits remains an important area for future investigations.

Circuit mechanisms underlying cholinergic-evoked network activity

Our finding showing that activation of BF inputs can lead to oscillatory activity in thalamic networks confirms that rhythmic activity is an "intrinsic" property of thalamic circuits and can be engaged by distinct synaptic afferents (Huguenard and McCor-

mick, 2007). Importantly, for thalamic oscillations triggered by the synchronous activation of CT feedback, disynaptic inhibition generated in VB neurons is at least partially opposed by monosynaptic excitation, because virtually all CT axons target both TRN and VB neurons simultaneously. Such an overlap of excitation and inhibition might be responsible for limiting thalamic oscillatory activity under normal conditions (Paz et al., 2011). In contrast, BF cholinergic afferents only activate one cell type of the oscillatory network and might therefore be more effective in engaging oscillatory activity in thalamic circuits.

Our studies highlight the rapid transformation of a near-synchronous activation of TRN neurons by BF inputs into asynchronous oscillatory thalamic activity. Previous work *in vivo* and *in vitro* has led to the identification of a number of possible mechanisms that could either enhance or reduce thalamic synchrony during oscillatory activity (Beenhakker and Huguenard, 2009). Specifically, the high synaptic divergence for both reticulothalamic and thalamoreticular connections, together with the presence of electrical coupling between TRN neurons, is assumed to enhance synchrony (Huguenard and McCormick, 2007), whereas local GABAergic connections between TRN neurons are thought to be critical in preventing generalized synchronization (Huntsman et al., 1999). Our present work points to several alternative cellular and circuit-based mechanisms that interact to prevent synchronous firing during thalamic oscillations.

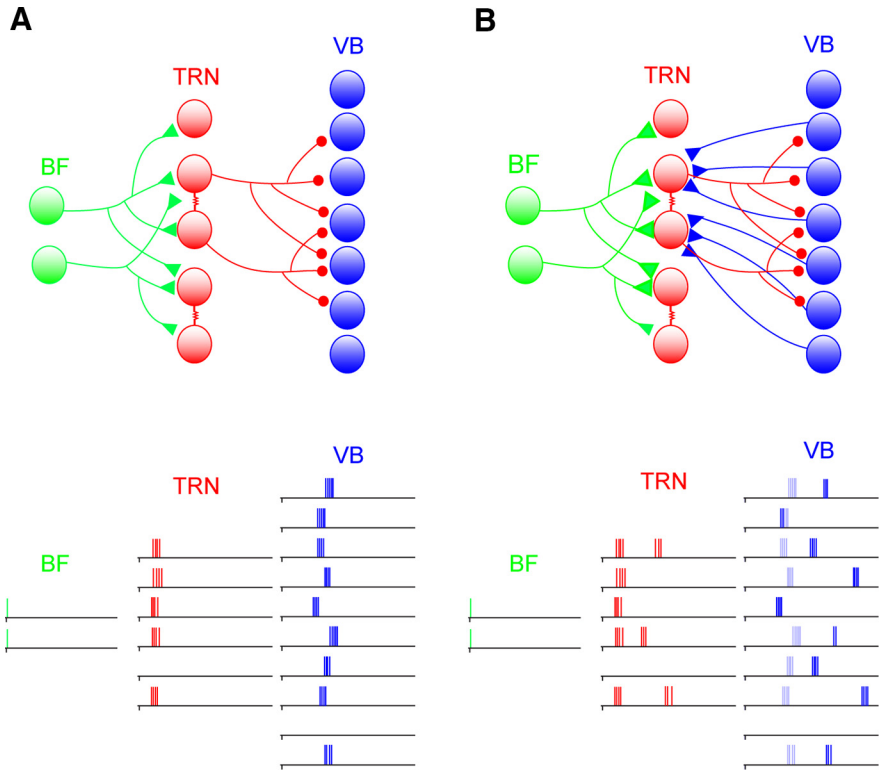

Figure 9. Multiple mechanisms interact to control cholinergic evoked thalamic network activity. ***A***, Top, Schematic representation of the isolated feedforward inhibitory network, indicating extensive divergence and convergence for both cholinergic inputs (green) to TRN and for reticulothalamic GABAergic connections (red). Bottom, Schematic of spike timing in the TRN (red) and VB (blue) in response to cholinergic activity (green), depicting the near-simultaneous activation of TRN neurons, leading to rebound bursting in VB neurons over a range of latencies. ***B***, Top, Schematic representation of the full thalamic network, including thalamoreticular connections (blue) that show little divergence in TRN. Bottom, Asynchronous activity in VB neurons generated by cholinergic-evoked feedforward inhibition (faint blue) is further desynchronized by the presence of lateral inhibition (blue). Persistent TRN neuronal activity is sparse and asynchronous (red). For details, see Discussion.

First, we found that neighboring VB neurons are the target of synaptic contacts originating from the same group of TRN neurons, resulting in synchronized inhibition. This extends anatomical work showing that individual TRN neurons form extensive axonal arborizations within sensory thalamic nuclei, often characterized by a single well circumscribed dense core containing a large number of putative terminals (Pinault and Deschênes, 1998a). Furthermore, divergence in reticulothalamic connectivity is accompanied by extensive convergence of multiple TRN neurons onto a given VB cell, based on the large IPSC amplitudes recorded in VB neurons.

Despite this anatomical arrangement and the resulting large and reliable inhibitory input to VB neurons, cholinergic-evoked rebound bursting had significant latency jitter from trial to trial, and burst firing in neighboring neurons never occurred synchronously. This suggests that even moderate variations in IPSP amplitude (attributable to fluctuations in release probability or TRN cell recruitment), together with fluctuations in postsynaptic membrane potential, will strongly influence burst latency in a given neuron. In addition, although the timing of IPSP bursts was virtually identical for neighboring neurons, their amplitudes and overall waveform showed significant differences, likely as a result of target cell-specific differences in dendritic location, number, and release properties of synaptic terminals. The strong dependence of burst latency on IPSC kinetics (Sohal et al., 2006) likely explains why APs in neighboring neurons were never synchronized (Fig. 9*A*).

Second, we found that lateral inhibition (Pinault and Deschênes, 1998b) plays a significant role in further desynchronizing VB cell firing (Fig. 9*B*). Although lateral inhibition features prominently in many neuronal circuit models (Karnani et al., 2014), its precise contribution to information processing has been difficult to characterize experimentally. In our case, we were able to quantify the influence of lateral inhibition because it was mediated by glutamatergic synapses that re-excite TRN GABAergic neurons, whereas the initial activation of VB cells required cholinergic and GABAergic synaptic activity. Importantly, the main consequence of lateral inhibition of cholinergic-evoked VB activity was an additional increase in spike jitter, accompanied by a moderate reduction in spike probability. In contrast, for VB neurons activated by sensory inputs, lateral inhibition mediated by TRN is expected to enhance precision, by enforcing brief temporal windows in which glutamatergic inputs can be integrated to generate neuronal output.

Third, we determined that individual thalamoreticular inputs to the TRN are powerful but sparse and contact only a limited number of postsynaptic TRN neurons (Fig. 9*B*), in contrast to current thalamic circuit models but in agreement with previous anatomical work (Pinault, 2004). Interestingly, even for TRN neurons with overlapping dendritic fields (as indicated by electrical synaptic coupling), we found very little evidence of shared

synaptic inputs. Because cholinergic-evoked activity in VB neurons was asynchronous, this led to the generation of independent patterns of excitatory synaptic inputs in neighboring TRN neurons. As a consequence, AP activity in neighboring TRN neurons was asynchronous, even under conditions of apamin-mediated enhanced oscillatory activity. Thus, the presence of electrical synapses in local clusters of TRN neurons (Long et al., 2004) does not appear to play a role in generating synchrony under these conditions.

Functional implications

Our findings suggest that activation of the cholinergic BF can control the processing of sensory information by transiently recruiting thalamic networks. Recent studies have indicated that cholinergic BF inputs to the neocortex act to desynchronize neuronal activity, leading to improved sensory perception (Pinto et al., 2013). The specific properties of BF-evoked thalamic modulation of sensory processing remain to be established. Sensory afferent activity can generate synchronous firing in local clusters of thalamic neurons with exquisitely high temporal precision (Bruno, 2011). However, the degree of thalamic synchrony can vary depending on stimulus features and the number of stimulus presentations (Temereanca et al., 2008). We suggest that BF inputs could similarly limit sensory-evoked correlated firing by generating synchronous inhibition in local clusters of thalamic neurons, with cell-specific inhibitory response magnitudes resulting in a range of latencies in spike timing. Such a fine tuning in the degree of synchrony might be critical for the detection and discriminability of sensory stimuli (Wang et al., 2010). At the same time, spatially restricted synchronous inhibition could be responsible for a correlated switch in firing mode in neighboring thalamic neurons, allowing for the generation of burst firing in local clusters of thalamic neurons (Swadlow and Gusev, 2001) but preventing widespread synchronous burst firing and the generation of epileptiform activity. More generally, our study emphasizes that thalamic circuits formed by TRN and VB neurons, long assumed to be involved in maintaining synchronous oscillations (Beenhakker and Huguenard, 2009), can in fact play a critical role in decorrelating afferent synaptic inputs, with important consequences for information processing.

References

Arroyo S, Bennett C, Aziz D, Brown SP, Hestrin S (2012) Prolonged disynaptic inhibition in the cortex mediated by slow, non-alpha7 nicotinic excitation of a specific subset of cortical interneurons. J Neurosci 32:3859–3864. CrossRef Medline

Beenhakker MP, Huguenard JR (2009) Neurons that fire together also conspire together: is normal sleep circuitry hijacked to generate epilepsy? Neuron 62:612–632. CrossRef Medline

Boucetta S, Cissé Y, Mainville L, Morales M, Jones BE (2014) Discharge profiles across the sleep-waking cycle of identified cholinergic, GABAergic, and glutamatergic neurons in the pontomesencephalic tegmentum of the rat. J Neurosci 34:4708–4727. CrossRef Medline

Bruno RM (2011) Synchrony in sensation. Curr Opin Neurobiol 21:701–708. CrossRef Medline

Bryant AS, Li B, Beenhakker MP, Huguenard JR (2009) Maintenance of thalamic epileptiform activity depends on the astrocytic glutamate-glutamine cycle. J Neurophysiol 102:2880–2888. CrossRef Medline

Chubykin AA, Roach EB, Bear MF, Shuler MG (2013) A cholinergic mechanism for reward timing within primary visual cortex. Neuron 77:723–735. CrossRef Medline

Descarries L, Gisiger V, Steriade M (1997) Diffuse transmission by acetylcholine in the CNS. Prog Neurobiol 53:603–625. CrossRef Medline

Gentet LJ, Ulrich D (2003) Strong, reliable and precise synaptic connections between thalamic relay cells and neurones of the nucleus reticularis in juvenile rats. J Physiol 546:801–811. CrossRef Medline

Gu Z, Yakel JL (2011) Timing-dependent septal cholinergic induction of dynamic hippocampal synaptic plasticity. Neuron 71:155–165. CrossRef Medline

Hallanger AE, Levey AI, Lee HJ, Rye DB, Wainer BH (1987) The origins of cholinergic and other subcortical afferents to the thalamus in the rat. J Comp Neurol 262:105–124. CrossRef Medline

Huguenard JR, McCormick DA (2007) Thalamic synchrony and dynamic regulation of global forebrain oscillations. Trends Neurosci 30:350–356. CrossRef Medline

Huntsman MM, Porcello DM, Homanics GE, DeLorey TM, Huguenard JR (1999) Reciprocal inhibitory connections and network synchrony in the mammalian thalamus. Science 283:541–543. CrossRef Medline

Karnani MM, Agetsuma M, Yuste R (2014) A blanket of inhibition: functional inferences from dense inhibitory connectivity. Curr Opin Neurobiol 26C:96–102. CrossRef Medline

Kolisnyk B, Guzman MS, Raulic S, Fan J, Magalhães AC, Feng G, Gros R, Prado VF, Prado MA (2013) ChAT-ChR2-EYFP mice have enhanced motor endurance but show deficits in attention and several additional cognitive domains. J Neurosci 33:10427–10438. CrossRef Medline

Lee MG, Hassani OK, Alonso A, Jones BE (2005) Cholinergic basal forebrain neurons burst with theta during waking and paradoxical sleep. J Neurosci 25:4365–4369. CrossRef Medline

Letzkus JJ, Wolff SB, Meyer EM, Tovote P, Courtin J, Herry C, Lüthi A (2011) A disinhibitory microcircuit for associative fear learning in the auditory cortex. Nature 480:331–335. CrossRef Medline

Levey AI, Hallanger AE, Wainer BH (1987) Cholinergic nucleus basalis neurons may influence the cortex via the thalamus. Neurosci Lett 74:7–13. CrossRef Medline

Long MA, Landisman CE, Connors BW (2004) Small clusters of electrically coupled neurons generate synchronous rhythms in the thalamic reticular nucleus. J Neurosci 24:341–349. CrossRef Medline

McCormick DA, Bal T (1997) Sleep and arousal: thalamocortical mechanisms. Annu Rev Neurosci 20:185–215. CrossRef Medline

Munoz W, Rudy B (2014) Spatiotemporal specificity in cholinergic control of neocortical function. Curr Opin Neurobiol 26C:149–160. CrossRef Medline

Parikh V, Kozak R, Martinez V, Sarter M (2007) Prefrontal acetylcholine release controls cue detection on multiple timescales. Neuron 56:141–154. CrossRef Medline

Paz JT, Bryant AS, Peng K, Fenno L, Yizhar O, Frankel WN, Deisseroth K, Huguenard JR (2011) A new mode of corticothalamic transmission revealed in the Gria4(−/−) model of absence epilepsy. Nat Neurosci 14:1167–1173. CrossRef Medline

Perkins KL (2006) Cell-attached voltage-clamp and current-clamp recording and stimulation techniques in brain slices. J Neurosci Methods 154:1–18. CrossRef Medline

Picciotto MR, Higley MJ, Mineur YS (2012) Acetylcholine as a neuromodulator: cholinergic signaling shapes nervous system function and behavior. Neuron 76:116–129. CrossRef Medline

Pinault D (2004) The thalamic reticular nucleus: structure, function and concept. Brain Res Brain Res Rev 46:1–31. CrossRef Medline

Pinault D, Deschênes M (1998a) Projection and innervation patterns of individual thalamic reticular axons in the thalamus of the adult rat: a three-dimensional, graphic, and morphometric analysis. J Comp Neurol 391:180–203. CrossRef Medline

Pinault D, Deschênes M (1998b) Anatomical evidence for a mechanism of lateral inhibition in the rat thalamus. Eur J Neurosci 10:3462–3469. CrossRef Medline

Pinto L, Goard MJ, Estandian D, Xu M, Kwan AC, Lee SH, Harrison TC, Feng G, Dan Y (2013) Fast modulation of visual perception by basal forebrain cholinergic neurons. Nat Neurosci 16:1857–1863. CrossRef Medline

Sohal VS, Pangratz-Fuehrer S, Rudolph U, Huguenard JR (2006) Intrinsic and synaptic dynamics interact to generate emergent patterns of rhythmic bursting in thalamocortical neurons. J Neurosci 26:4247–4255. CrossRef Medline

Sun YG, Pita-Almenar JD, Wu CS, Renger JJ, Uebele VN, Lu HC, Beierlein M (2013) Biphasic cholinergic synaptic transmission controls action potential activity in thalamic reticular nucleus neurons. J Neurosci 33:2048–2059. CrossRef Medline

Swadlow HA, Gusev AG (2001) The impact of "bursting" thalamic im-

pulses at a neocortical synapse. Nat Neurosci 4:402–408. CrossRef Medline

Temereanca S, Brown EN, Simons DJ (2008) Rapid changes in thalamic firing synchrony during repetitive whisker stimulation. J Neurosci 28: 11153–11164. CrossRef Medline

Thiele A (2009) Optimizing brain processing. Nat Neurosci 12:1359–1360. CrossRef Medline

Wang Q, Webber RM, Stanley GB (2010) Thalamic synchrony and the adaptive gating of information flow to cortex. Nat Neurosci 13:1534–1541. CrossRef Medline

Woolf NJ, Butcher LL (2011) Cholinergic systems mediate action from movement to higher consciousness. Behav Brain Res 221:488–498. CrossRef Medline

Wu CS, Zhu J, Wager-Miller J, Wang S, O'Leary D, Monory K, Lutz B, Mackie K, Lu HC (2010) Requirement of cannabinoid CB(1) receptors in cortical pyramidal neurons for appropriate development of corticothalamic and thalamocortical projections. Eur J Neurosci 32:693–706. CrossRef Medline

Zaborszky L (2002) The modular organization of brain systems. Basal forebrain: the last frontier. Prog Brain Res 136:359–372. CrossRef Medline

Zhao S, Ting JT, Atallah HE, Qiu L, Tan J, Gloss B, Augustine GJ, Deisseroth K, Luo M, Graybiel AM, Feng G (2011) Cell type-specific channelrhodopsin-2 transgenic mice for optogenetic dissection of neural circuitry function. Nat Methods 8:745–752. CrossRef Medline